Triton X-100 promotes a cholesterol-dependent condensation of the plasma membrane

Mercedes Ingelmo-Torres, Katharina Gaus, Albert Herms, Elena González-Moreno, Adam Kassan, Marta Bosch, Thomas Grewal, Francesc Tebar, Carlos Enrich, Albert Pol

HAL Id: hal-00479147
https://hal.science/hal-00479147

Submitted on 30 Apr 2010

TRITON X-100 PROMOTES A CHOLESTEROL-DEPENDENT CONDENSATION OF THE PLASMA MEMBRANE.

Mercedes Ingelmo-Torres[1], Katharina Gaus[2], Albert Herms[3], Elena González-Moreno[1], Adam Kassan[3], Marta Bosch[3], Thomas Grewal[4], Francesc Tebar[1], Carlos Enrich[1] and Albert Pol[3,5].

From Departament de Biologia Cel·lular. Facultat de Medicina. Universitat de Barcelona. Casanova 143. 08036 Barcelona[1], Centre for Vascular Research, University of New South Wales, Sydney, NSW 2052, Australia[2], Institut d'Investigacions Biomèdiques August Pi i Sunyer (IDIBAPS). Casanova 143. 08036 Barcelona[3], Faculty of Pharmacy, Department of Pharmaceutical Chemistry, University of Sydney. Sydney, NSW 2006, Australia[4] and Institució Catalana per a la Recerca i Estudis Avançats (ICREA)[5].

Running head: Triton condensates the plasma membrane.

Address correspondence to: Albert Pol, Departament de Biologia Cel·lular, Facultat de Medicina, Institut d'Investigacions Biomèdiques August Pi Sunyer (IDIBAPS), Universitat de Barcelona. Casanova 143. 08036-Barcelona; E-mail: **apols@ub.edu** .

Abstract

The molecular components of membrane rafts are frequently defined by the biochemical partitioning into detergent-resistant membranes. In this study, we used a combination of epifluorescence and two-photon microscopy to visualize and quantify whether the detergent insolubility reflects a pre-existing organization of the plasma membrane (PM). We found that treatment of cells with cold Triton X-100 (TX) promotes a profound remodelling of the PM including a rapid rearrangement of GM1 and cholesterol into newly formed structures, only partial solubilization of fluid domains and the formation of condensed domains that cover 51% of the remaining membrane. Rather than inducing the coalescence of pre-existing domains, the remaining domains after TX treatment appear to be newly formed with a higher degree of condensation than those observed in native membranes. However, when cholesterol was physically complexed with a second detergent, such as saponin, cholesterol did not separate into the newly formed structures, condensation of the domains was unaltered and the relative area corresponding to ordered domains increased to occupy 62% of the remaining membrane. Our results suggest that detergent can be used to enrich ordered domains for biochemical analysis but that TX treatment alone substantially alters the lateral organization of the PM.

Introduction

The lipid raft hypothesis proposes that cholesterol and sphingolipids segregate from glycerophospholipids and dynamically associate to form distinct liquid-ordered microdomains in a lipid bilayer [1, 2]. Once formed, membrane rafts could provide a temporal and spatial compartment for selected lipids and proteins and thus introducing specificity into processes such as signal transduction, cell migration and the dynamic sorting of membrane components [3-7]. Biologically, raft-mediated membrane sorting would offer the cell two unique properties to overcome the limitations that are demonstrated by the coat proteins-mediated sorting. Firstly, it drives the dynamic sorting of selected lipids into newly formed domains and vesicles; and secondly, it provides a mechanism for segregation of non-raft molecules away from specific trafficking pathways.

Probably due to their small size and transient nature, membrane rafts have been difficult to characterize in living cells. An important part of our current knowledge of their existence and function has been obtained by biophysical means or indirect techniques such as cold detergent extraction or acute cholesterol depletion. It is generally assumed that membrane rafts could be preferentially isolated by taking advantage of their unique insolubility in cold detergents such as Triton X-100 (TX) and consistent low buoyant density in sucrose gradients. Earlier electron microscopy observations of detergent resistant membranes (DRM) described these membrane fragments as a heterogeneous population of vesicles ranging from 0.1 to 1 μm in diameter containing GPI-anchored proteins [8]. Since then, it has been difficult to prove such PM organization in living cells. Recently, the poorly understood interaction between surfactants and the components of the membrane bilayer has led to the questioning to which extent DRM reflect the organization of the intact cell membrane [9-11]. For example, it was observed that raft composition differs substantially when isolated in the presence or absence of detergents [12] and depends on which detergents are used [13]. This apparent contradiction may be explained by the fact that treatment of liposomes with TX is sufficient to promote the formation of liquid-ordered domains, suggesting that detergent solubilisation could involve the formation of non-physiological structures [14-17]. However, results obtained from artificial membranes are difficult to extrapolate to living cells as the PM is made up of a complex mixture of lipids and proteins that combine to form the asymmetrical bilayer. Although DRM may not reflect the PM organization, the insolubility of lipids and proteins often establishes a preliminary link with membrane rafts. Indeed, DRM are still used to define raft affinity or preferential partitioning, most convincingly when changes in DRM composition can be promoted by physiological events [9].

Therefore, a detailed characterization of the interaction between surfactants and the asymmetrical bilayer remains as a fundamental question in the study of the organization of the PM. In this study we have combined epifluorescence and two-photon microscopy to visualize and quantify the remodelling of the PM of living cells by detergents in order to i) understand the action of TX on the cell membrane and ii) further the establishment of a detergent protocol that more accurately enriches in pre-existing raft domains.

3

Experimental Procedures

Cell culture and reagents. COS-7 cells were maintained in DMEM supplemented with 5 % v/v fetal calf serum, L-glutamine (2mM), penicillin (50U/ml) and streptomycin sulphate (50µg/ml)(Biological Industries, Israel). Filipin (F-9765), Triton X-100 (TX) and saponin (S-4521) were purchased from Sigma-Aldrich Corporation (Madrid, Spain). Cholera toxin subunit B conjugated to Alexa fluorophore 594 and secondary antibodies conjugated to Alexa fluorophores were from Molecular Probes Inc. (Netherlands). Rabbit polyclonal anti-CAV1 (C13630) was purchased from Transduction Laboratories (KY, USA). Protein was quantified using the Lowry method [18]. Cholesterol in cell lysates was quantified as described previously [19].

Detergent solubilisation. Cells (2.5×10^6) were plated (18h before the experiment) in a 10 cm dish (60 cm^2) that contained glass cover-slips of 1 cm in diameter (0.79 cm^2). At the time of the experiment each dish contained approximately 1140 µg of protein and 9.12 µg of cholesterol and thus each cover-slip contained approximately 15 µg of protein and 0.12 µg of cholesterol. Next, the cover-slips were inverted and washed in a cold tris-based buffer (5 mM Tris-HCl pH 7.5, 150 mM NaCl, 5 mM EDTA) and incubated at 4ºC in a 30 µl drop of a tris-based buffer that, where indicated, contained 1% TX or a combination of 1% TX and 0.05% saponin (freshly prepared prior to use). After different incubation periods (ranging from 10 sec to 30 min), the cover-slips were fixed for 10 min in 50 µl of 4% paraformaldehyde (PFA) at 4ºC and for an additional 50 min in 50 µl of 4% PFA at room temperature. In other experiments, cells were plated at low density (7.5×10^5 cells) and treated as described above.

Laurdan, filipin cholera toxin and CAV1 staining and imaging. The filipin staining of fixed cells was performed as described previously [20]. Briefly, after fixation with 4% PFA, the cover-slips were washed in PBS and incubated in 100 µl of PBS containing 5 µg/ml filipin (freshly prepared from a 5 mg/ml stock solution in DMSO stored at –80ºC) at room temperature for 30 min. For the GM1 detection, the cells were treated at 4ºC for 30 min with CO_2-independent medium (GIBCO, UK) containing 2 µg/ml of Alexa-594-conjugated cholera toxin subunit B (from a 2 mg/ml stock solution in water stored at -20ºC). Next, the cover-slips were treated with detergents as described above, fixed in 4% PFA and labelled with filipin. CAV-1 immunolabelling was performed as described previously [20]. In these experiments 5 µg/ml of filipin was added to the blocking solution and to the buffers of the primary and secondary antibodies. Finally, the cover-slips were mounted in Mowiol, prepared according to the manufacturer's instructions (Calbiochem, CA, USA). Cells were observed using an oil-immersion Plan-Apo63x/1.4 objective in a Axio-plan or Axiovert 200M Zeiss microscope (Zeiss, Göttingen, Germany). In the Axio-plan microscope, the images were captured with an AxioCam HRc camera and were digitally treated with AxioVision 3.1 software. In the 200M microscope the images were captured with a Photometrics Cool Snap HQ camera controlled by slide-book 3.0.10.5 software (Intelligent Imaging Innovation, CO, USA). Image analysis was performed with Adobe-Photoshop 5.5 software (Adobe Systems Inc.). Laurdan labelling of live and fixed cells and two-photon microscopy was performed using a DM IRE2 Microscope (Leica, Gladesville, Australia) as described previously [21]. In brief, Laurdan was excited at 800 nm and emission intensities simultaneously recorded in the range of 400-460 nm and 470-530 nm. Intensity images for each pixel were converted into Generalized Polarization (GP) images (WiT software) with:

4

$$GP = \frac{I_{(400\text{-}460)} - I_{(470\text{-}530)}}{I_{(400\text{-}460)} + I_{(470\text{-}530)}}$$

GP distributions were obtained from the histograms of GP images, normalized (sum = 100), and fitted to Gaussian distributions using the nonlinear fitting algorithm Solver (Microsoft Excel). Microscope calibrations were carried out as previously described [21-23]. The GP histograms were calculated from ~80 cells for each condition.

Results

Triton promotes the formation of new ordered domains in the plasma membrane We analysed the lipid structure of the cell surface of COS cells by means of two-photon microscopy. The fluorescent probe 6-acyl-2-dimethylaminonapthalene (Laurdan) has been used to characterize phase separation in model membranes [24, 25] and visualize ordered domains on the surface of living cells [21]. Laurdan does not preferentially partition into either lipid phase but undergoes a shift in its peak emission wavelength from 500 nm in fluid membranes to 440 nm in condensed membranes. We simultaneously recorded the Laurdan fluorescence intensity in two channels: 400–460 nm (condensed membranes) and 470–530 nm (fluid membranes). Then, for each pixel a normalized ratio of the two emission regions is given by the generalized polarization (GP). Next, the GP histograms are obtained from ~80 cells for each condition and the histogram fitted to two Gaussian populations providing us with the mean GP value of each population and their relative abundance or coverage. GP values range from –1 (very fluid) to +1 (very condensed) and measure membrane fluidity with fluid domains in the range of approximately –0.05 to 0.25 and ordered domains in a range of 0.25–0.55. Throughout this paper, we will refer to lipid rafts as the hypothesized entity and to domains as the areas within the cell membrane that were examined microscopically. Given the spatial resolution of light microscopy (~200 nm), it is therefore likely that lipid rafts are substantially smaller than the experimentally observed domains.

COS-7 cells on cover-slips (equivalent to 15 mg protein and 0.12 mg of cholesterol per cover-slip) were labelled with Laurdan. In Figure 1A-D, the resulting GP images are pseudo-coloured to show fluid membranes in green (GP<0.3) and ordered membranes in red to yellow (GP>0.3). At the cell surface, we found (Figure 1A) condensed domains (with a mean GP of 0.48-0.49±0.06) that occupied 22.7%±5.5% of the PM (black line in Figure 1E for the Gaussian distribution of the GPs and 1G for the mean GP and the relative coverage between fluid and condensed populations). After incubating the cells for 10 min (Figure 1B, red line in 1E and 1G) or 20 min in a cold buffer (Figure 1C, black line in 1F and 1H), the abundance of ordered domains was similar with a 23.2% or 20.1% respectively. Identical results for GP and relative coverage were obtained in fixed and living cells (not shown). Next, in order to quantify whether the insolubility of the PM in non-ionic detergents correlates to with its organization into ordered/fluid domains, 1% TX was added to the cells and the GP was analysed after 10 min. Interestingly, the addition of TX induced a dramatic shift in the mean GP of the ordered membrane population to 0.64±0.05 and condensed domains now covered 51.4%±5.5% of the cell membrane (Figure 1D, red line in 1F and 1H). Therefore, TX promoted two different processes: firstly it partially solubilised fluid domains of the PM (48.6% of the cell membrane remains in a fluid state with a GP of 0.079), and secondly it promoted the formation of highly ordered domains that are distinctly different from those in native membranes. The latter is demonstrated by the increase the mean GP from 0.493 to 0.639. Thus it is likely that condensed

5

regions are formed *de novo* rather than being the result of the coalescence of pre-existing domains. Whether these apparently new highly ordered domains are created by the coalescence of pre-existing membrane rafts that are below the resolution of the microscope cannot be resolved with this approach. In model membranes, GP values of >0.6 typically signify gel phases rather than ordered phases. Thus, it unlikely that pre-existing rafts are responsible for such a dramatic membrane condensation. It is however remarkable that highly ordered domains were generally formed in regions in which the cell membrane already presented a relatively high degree of condensation (compare Figures 1C and 1D), suggesting the possibility that lipids and/or proteins dynamically redistribute into already condensed regions of the membrane (see Discussion).

Visualization of cholesterol-enriched domains at the cell surface of COS cells. Highly-ordered domains are characterized by an increased concentration of cholesterol when compared with the bulk of the PM. Cholesterol-enriched domains have proven difficult to visualize in the PM of living cells [26]. However, by conventional fluorescence microscopy of chemically fixed cells, non-esterified free cholesterol is conveniently detected using filipin as a fluorescent marker [27-29]. In COS cells, filipin labelling was found in the Golgi/recycling endosomal area, PM and scattered intracellular vesicles [30]. We observed that in the PM, although widely distributed, cholesterol (similarly to ordered domains detected by Laurdan) accumulated in regions of contact between neighbouring membranes (arrows in Figures 2A, 2B and 2C). In addition, strong labelling was detected close to the edge of the cell, forming a peripheral cortex of approximately 1.5-2 μm (arrowheads in Figures 2A, 2B and 2C). An identical distribution of filipin was observed when the cells were fixed with a combination of 4% PFA and 0.1% glutaraldehyde or when cells were fixed for 1h at 4ºC to reduce the possibility of clustering and/or extraction of lipids and proteins during the fixation protocol (data not shown). At high magnification, numerous filipin-enriched domains were prominent within the membrane (Figures 2B and 2C). Thus, taking into account the optical resolution and the limitations of filipin for detection of free cholesterol, the discontinuous distribution of filipin labelling may be consistent with the existence of distinct cholesterol-enriched domains in the PM. The filipin-enriched domains were generally round in shape, with an apparent average diameter of 253.3 nm ($\pm$ 44.5) and occupied 28.63% ($\pm$ 13.3) of the cell surface. This is similar to the coverage of ordered domains shown by Laurdan (22.7%).

To validate the use of filipin for the overall visualization of free cholesterol at the cell surface, we investigated whether filipin colocalises with two well-defined markers of membrane rafts: the glycosphingolipid GM1 and the protein caveolin-1 (CAV1). The B subunit of Cholera toxin (CTB), which binds to the glycosphingolipid GM1 in the PM, is hypothesized to be enriched in membrane rafts [31-33]. When cells were incubated with CTB at 4ºC, the toxin appeared widely distributed within the PM (Figures 2D and 2E for a high magnification of selected areas). Although an overlap with filipin was evident (arrowheads in Figures 2D and 2E), GM1 showed a more diffuse distribution and was not exclusively located to filipin-stained domains. We next analysed whether filipin colocalises with CAV1. In COS cells CAV1 was detected in the Golgi complex and in a punctate pattern in the PM (Figures 2F and 2G). In contrast to filipin, CAV1 was not accumulated at the edge of the cells and showed a less homogeneous distribution. Whilst at high magnification some of the filipin-enriched domains colocalised with CAV1 (arrows in Figure 1G), most did not, suggesting the existence of different subpopulations of cholesterol-enriched domains.

Triton promotes the reorganization of cholesterol in the plasma membrane. As shown above by means of Laurdan, TX promotes the formation of highly ordered domains. To determine

whether a similar redistribution of cholesterol occurs upon TX treatment, COS cells solubilised with 1% TX at 4ºC were labelled with filipin. After a very short treatment (30 sec), the pattern of cholesterol-rich domains lost its homogeneous distribution to form a network of tubular aggregates that occupied the entire membrane (compare Figures 3A and 3B). After 10 min the membrane appeared fenestrated (Figure 3C), with numerous holes surrounded by a ring of cholesterol (Figure 3C'). In the remaining membrane, cholesterol formed discrete ring-like (arrows in Figure 3C'), tubular and rounded structures that coexisted with filipin-negative domains. No significant changes were observed with longer incubations. Other authors have described similar TX-induced "Swiss cheese"-like morphologies of putative raft proteins [34, 35]. Under these experimental conditions, 26.2% (±3.3) of the total cellular protein was resistant to the TX extraction. In contrast, 70.2% (±6.6) of the cellular cholesterol was resistant to the detergent. When fewer cells (equivalent to approximately 5 μg protein and 0.04 μg of cholesterol per cover-slip) were incubated with the same volume of detergent, cholesterol was not observed in discrete aggregates but instead formed a homogeneous fenestrated sheet (Figures 3D and 3D') indicative of the importance of the mole ratio between detergents and membranes during the extraction. In addition, it is possible that changes in the concentration of proteins within the solubilised membranes significantly modify the effective detergent:lipid mole ratio required for micellization. In conclusion, these results demonstrate that, rather than a simple solubilisation of specific domains, TX promotes the reorganization and aggregation of cholesterol into newly formed structures of the PM.

Triton promotes the reorganization of GM1 but not CAV1 in the plasma membrane. Glycosphingolipids and sphingomyelin segregate from glycerophospholipids independently of other lipids or cholesterol [36]. To elucidate whether sphingolipids co-segregate with cholesterol in response to TX, we studied the effect of the detergent on GM1. After incubation of the cells with TX for 10 min, GM1 and cholesterol were detected in the same domains of the PM (Figures 4A and 4B for a high magnification). This is in contrast to untreated cells where only a partial colocalisation was observed. After TX treatment, the overlap was visible in the majority of the membrane and, at high magnification, in the tubular aggregates of cholesterol (arrows in Figure 4B). The labelling of GM1 appeared more diffuse when compared with filipin, probably reflecting that whereas filipin intercalates within cholesterol-enriched membranes, the CTB binds to GM1 on the PM. The increased colocalization between cholesterol and GM1 was confirmed and quantified by the Pearson correlation equation that shifts from 0.36±0.1 in untreated cells to 0.80±0.05 in the cells treated with TX (average calculated from the analysis of 65 cells). In contrast to cholesterol and GM1, CAV1 distribution in the PM was almost unaffected by treatment with TX (compare Figure 2F with Figure 4C). Although some CAV1 was found in the newly formed cholesterol domains, at high magnification very little colocalisation was observed and instead CAV1 accumulated at the edges of the holes (arrows in Figure 4D). It is generally accepted that the pool of CAV1 at the cell surface is relatively immobile unless the cells are perturbed experimentally [37-40], making CAV1 a good marker for stable PM-associated cholesterol enriched domains. Thus, the results shown here may indicate that a preformed lipid domain, whilst being unaffected by extraction with detergent, is displaced during the remodelling of the PM with TX. In contrast to CAV1 and GM1, under the experimental conditions used here, a non-raft protein such as the transferrin receptor was completely solubilised by the detergent (data not shown).

Role of cholesterol in the Triton-induced reorganisation of the plasma membrane. So far, we have demonstrated that TX promotes the formation of ordered domains and the clustering of cholesterol and GM1 in the PM without affecting the distribution of CAV1. This prompted us to look for a biochemical method to prevent such reorganization without affecting preformed

ordered domains. It has been previously described that some GPI-proteins are almost, but not completely, soluble when cells are treated with saponin, to complex cholesterol, prior to extraction with TX [41, 42]. In contrast, CAV1 is highly resistant to the extraction with saponin (not shown). Taking these precedents into account, we hypothesized that saponin could complex cholesterol and consequently prevent its clustering in response to TX treatment.

Therefore, COS cells were treated for 10 min with a combination of 1% TX and 0.05% saponin (TX/sap) and the distribution of cholesterol, GM1, and CAV1 was analysed. The combination of detergents did not induce formation of the characteristic holes in the PM observed after TX solubilisation (Figures 5A, 5B and 5C). Cholesterol was restricted to discrete rounded structures, frequently connected by tubular elements, which co-existed with filipin-negative domains. The filipin-enriched domains resembled in shape and size those described in untreated cells (compare Figures 5C and 2C). In addition, some of the filipin-enriched domains overlapped with CTB (Figures 5D and 5E). The Pearson correlation analysis confirmed the increased colocalisation between cholesterol and GM1 in response to TX/sap (0.66±0.6 in contrast to 0.36±0.1 in untreated cells) although it was markedly lower than the colocalisation shown after solubilisation with TX (0.80±0.05). In addition, in contrast to the treatment with TX, CAV1 was not excluded from the filipin-enriched domains (Figures 5F and 5G). Under these experimental conditions, 29% (±7.5) of the protein and 59.7% (±9.5) of cellular cholesterol (compared to 70.2% in TX-treated cells) was resistant to extraction with TX/sap. Finally, we studied the TX/sap-mediated solubilisation of cells by means of two-photon microscopy. Interestingly, the addition of TX/sap for 10 min to the cells (red line in Figure 5H) did not modify the mean GP of condensed domains (0.47), but increased considerably its relative enrichment at the cell membrane (to 61.9%)(table in Figure 5H). Therefore, in contrast to the solubilisation mediated by TX, the mixture of detergents do not alter the condensation of ordered domains although efficiently solubilises fluid domains.

Discussion

The core of the raft concept proposes that there is a lipid-driven segregation of membrane components to form distinct domains. Raft lipids, particularly glycosphingolipids and cholesterol, may pack tightly together and promote an active separation of other lipids such as glycerophospholipids. In this study we have visualized how cold TX promotes a similar, although artificial, lateral segregation of domains in the PM of COS cells.

Insolubility in cold TX has been often used as the biochemical criterion to define the existence and function of lipid raft components. Indeed, DRM were considered as the isolated cellular fraction equivalent to membrane rafts. Although it is clear that DRM do not reflect the organization of the PM, the insolubility of lipids and proteins in cold detergents identifies a potential link of these molecules with membrane rafts. Indeed, a non-raft protein such as the transferrin receptor is completely solubilised by TX. However, in the present study we have observed that TX induces a profound remodelling of the PM. In response to TX cholesterol and GM1 re-located and clustered into new structures inducing the formation of holes at the cell surface. We demonstrate that TX partially solubilises fluid domains (48.6% of the cell membrane remains in a fluid state with a GP of 0.079) and promotes the formation of new highly ordered domains (with a new GP of 0.64) which were absent in native membranes. These results clearly suggest that molecules with raft-affinity dynamically redistribute in response to the detergent to condense domains. After incubation with TX, GM1 and cholesterol showed a high degree of colocalization, which was not observed in untreated cells. Whether

these apparently new, highly ordered domains are created by the coalescence of pre-existing membrane rafts that are below the resolution of the microscope cannot be resolved. However, it seems unlikely that pre-existing rafts are responsible for the dramatic membrane condensation seen here. Heerklotz and co-workers [16] have shown that sphingomyelin-rich domains present in model membranes containing phosphatidylcholine-sphingomyelin-cholesterol (1:1:1, mol) are only marginally stable. The slight perturbation of the membrane by 0.2 kJ/mol that is caused by the addition of TX induces substantial domain formation in a previously homogeneous membrane but in addition it may change the composition of pre-existing domains. Interestingly, the degree of solubilisation also depends on the cell to detergent ratio, possibly reflecting that the saturating critical ratio (in which solubilisation begins and detergent-rich micelles form) is determined by lipids and by the presence of proteins within the solubilised membranes. It is remarkable that in response to TX highly ordered domains generally formed in regions in which the cell membrane already presented a relatively high degree of condensation. As the PM is made up of a complex mixture of lipids and proteins it is possible to hypothesize about the presence of naturally occurring raft stabilizers/raft promoters that may favour the TX-induced domain formation in specific regions of the asymmetrical bilayer. In this context, the role of the highly insoluble cortical actin as a determinant for raft 'nucleation sites' is an interesting concept that deserves further attention. In fact, the distribution of CAV1 at the cell surface was unchanged by TX, suggesting that caveolae are apparently unaffected by extraction with the detergent. However, a more detailed biochemical analysis will be required to characterize how detergents promote further condensation or modify the lipid/protein composition of caveolae.

When cholesterol is physically complex by saponin our results show that lipid clustering and hole formation is inhibited, cholesterol accumulates in structures that resemble their original domains in location, shape and size, and CAV1 colocalises with the remaining filipin-enriched domains. In addition, the combination of detergents does not promote the formation of new condensed domains, but efficiently solubilises fluid domains at the cell surface. In contrast to TX-extracted cells (70%), only 59.7% of the cellular free cholesterol was insoluble to TX/sap. Accordingly, we managed to establish that saponin treatment inhibits the TX-induced remodelling of the PM [34]. In agreement, the degree of condensation of the insoluble domains was unaffected by the mixture of detergents (GP of 0.47) but the relative area corresponding to condensed domains increased from 22% to 62%. It is then clear that the ability to partition into insoluble domains in the presence of TX reflects a potential affinity for ordered domains. In addition, the ability to partition into insoluble domains in the presence of TX/sap may provide a supplementary biochemical criterion to define stable and ordered domains at the PM. For example, as commented above, it has been described that some GPI-proteins are almost, but not completely, soluble when cells are treated with saponin, to complex cholesterol, prior to extraction with TX [41, 42]. Further investigation will be necessary to determine whether the molecules with affinity to associate with DRM maintain the capability to aggregate into the newly formed domains in the absence of cholesterol. In fact, detergent resistant membranes can be isolated from membranes lacking cholesterol [43, 44]. However, some authors have described a differential redistribution of GPI-anchored proteins from DRM into the TX-soluble fractions in response to the acute depletion of cholesterol [4, 45, 46]. In various cell types, the ceramide moiety of GM1 determines whether the molecular variants of the glycosphingolipid require cholesterol to fractionate into DRM [47].

In conclusion, the use of TX for studying stable lipid domains at the cell surface should be carefully interpreted and necessarily complemented with high-resolution methodologies. We propose that the use of mixtures of detergents with different solubilisation and/or fixation

9

properties could provide an additional biochemical criterion for the study of stable and ordered domains at the PM.

10

References

1   Simons, K. and Ikonen, E. (1997) Functional rafts in cell membranes. Nature **387**, 569-572

2   Hancock, J. F. (2006) Lipid rafts: contentious only from simplistic standpoints. Nat. Rev. Mol. Cell Biol. **7**, 456-462

3   Anderson, R. G. and Jacobson, K. (2002) A role for lipid shells in targeting proteins to caveolae, rafts, and other lipid domains. Science **296**, 1821-1825

4   Edidin, M. (2003) The state of lipid rafts: from model membranes to cells. Annu. Rev. Biophys. Biomol. Struct. **32**, 257-283

5   Maxfield, F. R. (2002) Plasma membrane microdomains. Curr. Opin. Cell Biol. **14**, 483-487

6   Munro, S. (2003) Lipid rafts: elusive or illusive? Cell **115**, 377-388

7   van Meer, G. (2004) Invisible rafts at work. Traffic 5, 211-212

8   Brown, D. A. and Rose, J. K. (1992) Sorting of GPI-anchored proteins to glycolipid-enriched membrane subdomains during transport to the apical cell surface. Cell **68**, 533-544

9   Lingwood, D. and Simons, K. (2007) Detergent resistance as a tool in membrane research. Nat. Protoc. **2**, 2159-2165

10   Zurzolo, C., van Meer, G. and Mayor, S. (2003) The order of rafts. Conference on microdomains, lipid rafts and caveolae. EMBO Rep. **4**, 1117-1121

11   Lichtenberg, D., Goni, F. M. and Heerklotz, H. (2005) Detergent-resistant membranes should not be identified with membrane rafts. Trends Biochem. Sci. **30**, 430-436

12   Pike, L. J., Han, X., Chung, K. N. and Gross, R. W. (2002) Lipid rafts are enriched in arachidonic acid and plasmenylethanolamine and their composition is independent of caveolin-1 expression: a quantitative electrospray ionization/mass spectrometric analysis. Biochemistry **41**, 2075-2088

13   Chamberlain, L. H. (2004) Detergents as tools for the purification and classification of lipid rafts. FEBS Lett. **559**, 1-5

14   de Almeida, R. F., Fedorov, A. and Prieto, M. (2003) Sphingomyelin/phosphatidylcholine/cholesterol phase diagram: boundaries and composition of lipid rafts. Biophys. J. **85**, 2406-2416

15   Heerklotz, H. (2002) Triton promotes domain formation in lipid raft mixtures. Biophys. J. **83**, 2693-2701

16   Heerklotz, H., Szadkowska, H., Anderson, T. and Seelig, J. (2003) The sensitivity of lipid domains to small perturbations demonstrated by the effect of Triton. J. Mol. Biol. **329**, 793-799

17   Sot, J., Collado, M., Arrondo, J., Alonso, A. and Goñi, F. (2002) Triton X-100 resistant bilayers: effect of lipid composition and relevante to the raft phenomenon. Langmuir **18**, 2828-2835

18   Lowry, O. H., Rosebrough, N. J., Farr, A. L. and Randall, R. J. (1951) Protein measurement with the Folin phenol reagent. J. Biol. Chem. **193**, 265-275

19   Rudel, L. L. and Morris, M. D. (1973) Determination of cholesterol using o-phthalaldehyde. J. Lipid Res. **14**, 364-366

20   Pol, A., Luetterforst, R., Lindsay, M., Heino, S., Ikonen, E. and Parton, R. G. (2001) A caveolin dominant negative mutant associates with lipid bodies and induces intracellular cholesterol imbalance. J. Cell Biol. **152**, 1057-1070

21   Gaus, K., Gratton, E., Kable, E. P., Jones, A. S., Gelissen, I., Kritharides, L. and Jessup, W. (2003) Visualizing lipid structure and raft domains in living cells with two-photon microscopy. Proc. Natl. Acad. Sci. U.S.A. **100**, 15554-15559

22   Gaus, K., Chklovskaia, E., Fazekas de St Groth, B., Jessup, W. and Harder, T. (2005) Condensation of the plasma membrane at the site of T lymphocyte activation. J. Cell Biol. **171**, 121-131

23   Gaus, K., Le Lay, S., Balasubramanian, N. and Schwartz, M. A. (2006) Integrin-mediated adhesion regulates membrane order. J. Cell Biol. **174**, 725-734

24   Bagatolli, L. A. and Gratton, E. (1999) Two-photon fluorescence microscopy observation of shape changes at the phase transition in phospholipid giant unilamellar vesicles. Biophys. J. **77**, 2090-2101

25   Dietrich, C., Volovyk, Z. N., Levi, M., Thompson, N. L. and Jacobson, K. (2001) Partitioning of Thy-1, GM1, and cross-linked phospholipid analogs into lipid rafts reconstituted in supported model membrane monolayers. Proc. Natl. Acad. Sci. U.S.A. **98**, 10642-10647

26   Mobius, W., Ohno-Iwashita, Y., van Donselaar, E. G., Oorschot, V. M., Shimada, Y., Fujimoto, T., Heijnen, H. F., Geuze, H. J. and Slot, J. W. (2002) Immunoelectron microscopic localization of cholesterol using biotinylated and non-cytolytic perfringolysin O. J. Histochem. Cytochem. **50**, 43-55

27   Kinsky, S. (1970) Antibiotic interaction with model membranes. Annu. Rev. Pharmacol. **10**, 119-142

28   Montesano, R. (1979) Inhomogeneous distribution of filipin-sterol complexes in the ciliary membrane of rat tracheal epithelium. Am. J. Anat. **156**, 139-145

29   Severs, N. J. and Simons, H. L. (1983) Failure of filipin to detect cholesterol-rich domains in smooth muscle plasma membrane. Nature **303**, 637-638

30   Holtta-Vuori, M., Tanhuanpaa, K., Mobius, W., Somerharju, P. and Ikonen, E. (2002) Modulation of cellular cholesterol transport and homeostasis by Rab11. Mol. Biol. Cell **13**, 3107-3122

31   Mayor, S. and Riezman, H. (2004) Sorting GPI-anchored proteins. Nat. Rev. Mol. Cell Biol. **5**, 110-120

32   Nichols, B. J. (2003) GM1-containing lipid rafts are depleted within clathrin-coated pits. Curr. Biol. **13**, 686-690

33   Sandvig, K. and van Deurs, B. (2002) Transport of protein toxins into cells: pathways used by ricin, cholera toxin and Shiga toxin. FEBS Lett. **529**, 49-53

34   Kenworthy, A. K., Nichols, B. J., Remmert, C. L., Hendrix, G. M., Kumar, M., Zimmerberg, J. and Lippincott-Schwartz, J. (2004) Dynamics of putative raft-associated proteins at the cell surface. J. Cell Biol. **165**, 735-746

35   Mayor, S. and Maxfield, F. R. (1995) Insolubility and redistribution of GPI-anchored proteins at the cell surface after detergent treatment. Mol. Biol. Cell **6**, 929-944

36   Mattjus, P., Kline, A., Pike, H. M., Molotkovsky, J. G. and Brown, R. E. (2002) Probing for preferential interactions among sphingolipids in bilayer vesicles using the glycolipid transfer protein. Biochemistry **41**, 266-273

37   Parton, R. G., Joggerst, B. and Simons, K. (1994) Regulated internalization of caveolae. J. Cell Biol. **127**, 1199-1215

38   Pelkmans, L., Kartenbeck, J. and Helenius, A. (2001) Caveolar endocytosis of simian virus 40 reveals a new two-step vesicular-transport pathway to the ER. Nat. Cell Biol. **3**, 473-483

39   Pelkmans, L., Puntener, D. and Helenius, A. (2002) Local actin polymerization and dynamin recruitment in SV40-induced internalization of caveolae. Science **296**, 535-539

40   Thomsen, P., Roepstorff, K., Stahlhut, M. and van Deurs, B. (2002) Caveolae are highly immobile plasma membrane microdomains, which are not involved in constitutive endocytic trafficking. Mol. Biol. Cell **13**, 238-250

41   Cerneus, D. P., Ueffing, E., Posthuma, G., Strous, G. J. and van der Ende, A. (1993) Detergent insolubility of alkaline phosphatase during biosynthetic transport and endocytosis. Role of cholesterol. J. Biol. Chem. **268**, 3150-3155

42   Schroeder, R. J., Ahmed, S. N., Zhu, Y., London, E. and Brown, D. A. (1998) Cholesterol and sphingolipid enhance the Triton X-100 insolubility of glycosylphosphatidylinositol-anchored proteins by promoting the formation of detergent-insoluble ordered membrane domains. J. Biol. Chem. **273**, 1150-1157

43   Hansen, G. H., Immerdal, L., Thorsen, E., Niels-Christiansen, L. L., Nystrom, B. T., Demant, E. J. and Danielsen, E. M. (2001) Lipid rafts exist as stable cholesterol-independent microdomains in the brush border membrane of enterocytes. J. Biol. Chem. **276**, 32338-32344

44   Milhiet, P. E., Giocondi, M. C. and Le Grimellec, C. (2002) Cholesterol is not crucial for the existence of microdomains in kidney brush-border membrane models. J. Biol. Chem. **277**, 875-878

45   Ilangumaran, S. and Hoessli, D. C. (1998) Effects of cholesterol depletion by cyclodextrin on the sphingolipid microdomains of the plasma membrane. Biochem. J. **335** (Pt 2), 433-440

46   Ostermeyer, A. G., Beckrich, B. T., Ivarson, K. A., Grove, K. E. and Brown, D. A. (1999) Glycosphingolipids are not essential for formation of detergent-resistant membrane rafts in melanoma cells. methyl-beta-cyclodextrin does not affect cell surface transport of a GPI-anchored protein. J. Biol. Chem. **274**, 34459-34466

47   Panasiewicz, M., Domek, H., Hoser, G., Kawalec, M. and Pacuszka, T. (2003) Structure of the ceramide moiety of GM1 ganglioside determines its occurrence in different detergent-resistant membrane domains in HL-60 cells. Biochemistry **42**, 6608-6619

Abbreviations

CAV1, caveolin-1; CTB, B subunit of cholera toxin; DRM, detergent resistant membranes; GM1, glycosphingolipid GM1; GP, general polarization index; PFA, paraformaldehyde; PM, plasma membrane; TX, triton X-100; TX/Sap, mixture of 1% triton X-100 and 0.05% saponin.

FIGURE LEGENDS

Figure 1. Laurdan labelling of TX-solubilised cells. (A-D) COS cells were labelled with Laurdan (A) and imaged for an additional 10 min (B) and 20 min (C) in ice-cold Tris buffer. After 20 min (C) the cells were additionally treated with 1% TX for 10 min and finally imaged (D). GP images were calculated from intensity images (see Materials and methods) and pseudocoloured with blue to yellow representing low to high GP values, respectively (see colour scale between panels C and D). (E-G) COS cells (black lines in E and F) were incubated for 10 min in ice-cold buffer (red line in E) or for 10 min in 1% TX (red line in F), labelled with Laurdan and the general polarization (GP) calculated. Pixel intensities were normalized and fitted to Gaussian populations (E and F). The corresponding mean GP of ~80 cells per conditions and the relative coverage between fluid and condensed populations were quantified (G and H). Average standard deviation of mean GP values for fluid and condensed populations are 0.06 and 0.05, respectively. Average standard deviation of coverage is 5.5%. Scale bars: A-D = 20 μm and high magnification panels = 5 μm.

Figure 2. Filipin staining reveals cholesterol-enriched domains in the PM of COS cells. (A-C) COS cells were fixed in PFA and incubated with filipin to detect free cholesterol. Note that although filipin is visible in the UV channel of the microscope, here it is shown in white or green to provide better visual resolution. Cholesterol is widely distributed in the PM but accumulates in a peripheral cortex (arrowheads) and at points of contact between neighbouring cells (arrows). In addition, numerous rounded, filipin-enriched domains are apparent within the membrane. (D and E) For the detection of GM1, cells were incubated CTB-Alexa 594, fixed in PFA and labelled with filipin. CTB (red channel) appear widely distributed in the PM. Although there is a clear overlap with cholesterol (arrowheads), GM1 shows a more diffuse distribution and GM1 is not exclusively located to filipin-stained domains (E, arrows). (F-G) Cells were fixed and labelled with filipin (green channel) and with an anti-CAV1 antibody (red channel). Filipin and CAV1 partially colocalise (arrows). Scale bars: A, D and F = 20 μm; B, C, E and G = 5 μm.
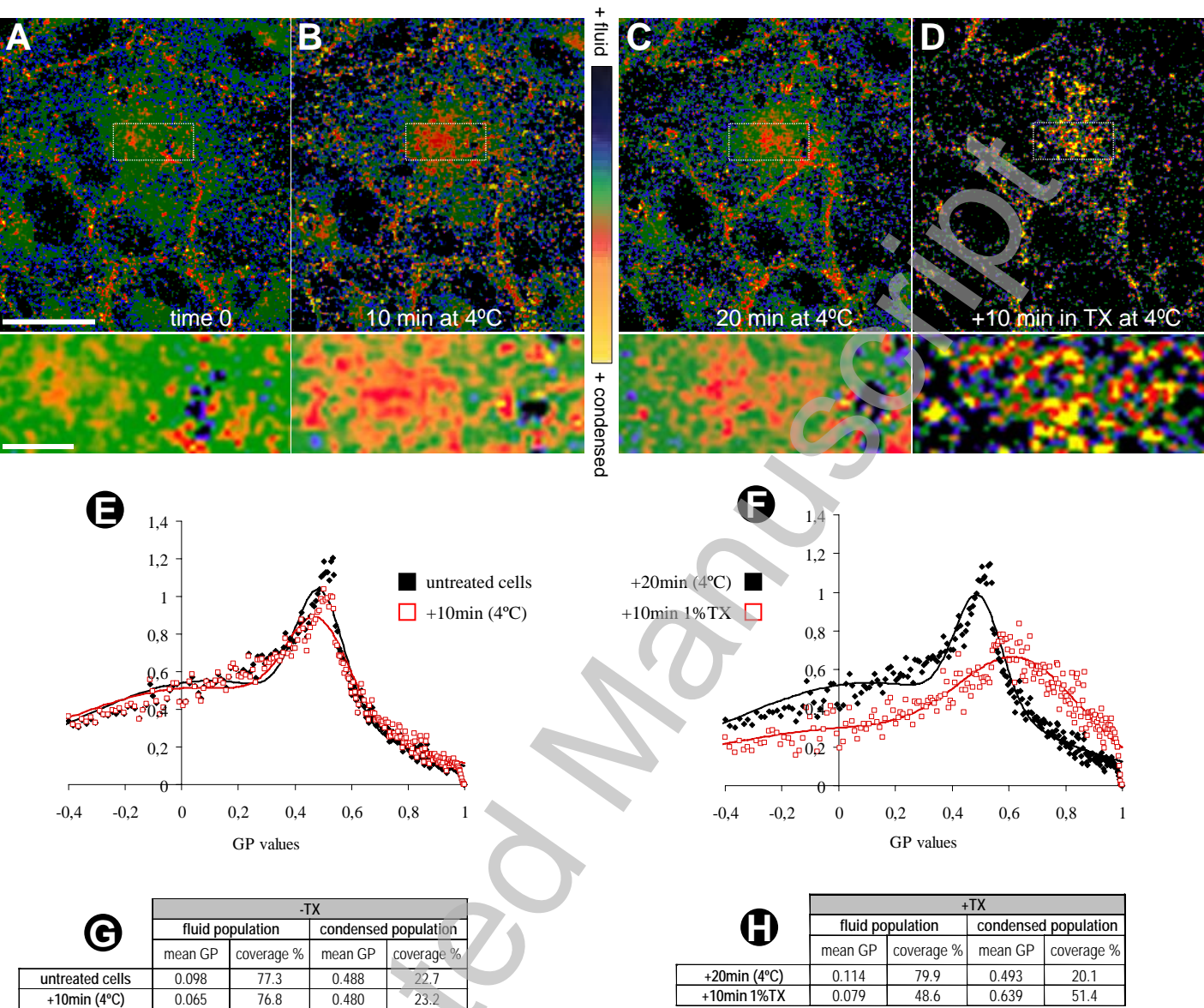
Figure 3. TX promotes the reorganization of cholesterol in the PM. COS cells growing on glass cover-slips were incubated at 4°C for up to 10 min in buffer containing 1% TX, then cells were fixed in PFA and incubated with filipin to detect free cholesterol. In contrast to untreated cells (A), after 30 sec (B) the pattern of cholesterol-rich domains lost its homogeneous distribution to form a network of tubular aggregates. After 10 min with the detergent (C and C'), numerous holes delimited by a ring of cholesterol appear on the cell surface and cholesterol form discrete tubulo-vesicular structures (arrows and arrowheads in C'). Squares indicate selected area for the high magnification panels. No changes are observed when the extraction is prolonged for more than 10 min. (D) Cells at low density were extracted for 10 min and then fixed and incubated with filipin. Cholesterol was not observed in discrete aggregates but instead formed a homogeneous fenestrated sheet. Scale bars: A-D = 20μm; C'-D' = 5 μm.

Figure 4. GM1, but not CAV1, reorganises in response to TX. (A, B) COS cells were incubated with CTB-Alexa 594, solubilised with 1% TX for 10 min, fixed in PFA and labelled with filipin. After extraction with the detergent, GM1 (red) and cholesterol (green) are detected in the same domains of the PM (A), colocalisation is observed in the bulk of the membrane and in tubular aggregates (arrows in B). (C, D) COS cells were solubilised with 1% TX, fixed in PFA and labelled with filipin (green) and with the anti-CAV1 antibody (red). CAV1 distribution is largely unaffected by treatment with TX (compare Figure 2F with 4C). When

14

observed at high magnification, CAV1 is excluded from the cholesterol-enriched domains formed in response to TX (arrows in D). Scale bars: A, C = 20 μm; B,D = 5 μm.
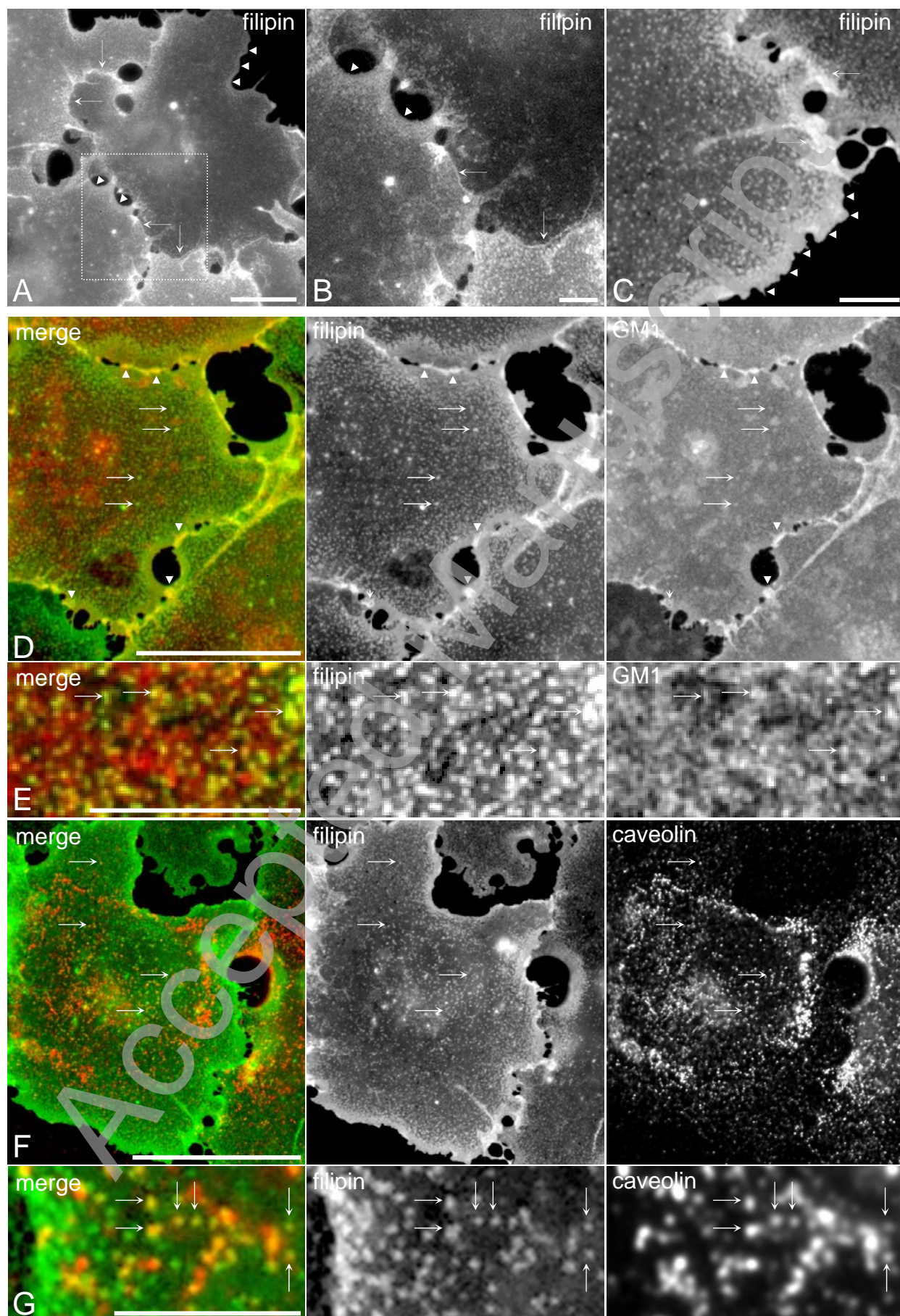
Figure 5. The presence of saponin inhibits the TX-induced aggregation of cholesterol and GM1. (A-C) Cells were solubilised with TX/sap for 10 min, fixed in PFA, and incubated with filipin. Cholesterol aggregates in discrete tubulo-vesicular structures that resemble in shape and size those described in untreated cells (compare A, B, and C with Figures 1A, B and C). (D,E) Cells were incubated with CTB, solubilised for 10 min with TX/sap, fixed with PFA and labelled with filipin. CTB colocalises with some of the tubulo-vesicular filipin-enriched structures (arrows in D and E). (F,G) TX/sap-treated and fixed cells were incubated with filipin and labelled with anti-CAV1 antibodies. CAV1 partially colocalises with filipin labelling (arrows in G). (H) COS cells (black lines) were incubated for 10 min in TX/sap (red line) and then labelled with Laurdan and the general polarization (GP) calculated as described in Figure 1. The addition of TX/sap to the cells did not modify the mean GP of condensed domains (0.47), but increases from 22.1% to 61.9% its relative enrichment at the cell membrane. Average standard deviation of mean GP values for fluid and condensed populations are 0.06 and average standard deviation of coverage is 5.5%. Scale bars: A-C, D and F = 20 μm; E, G = 5 μm.
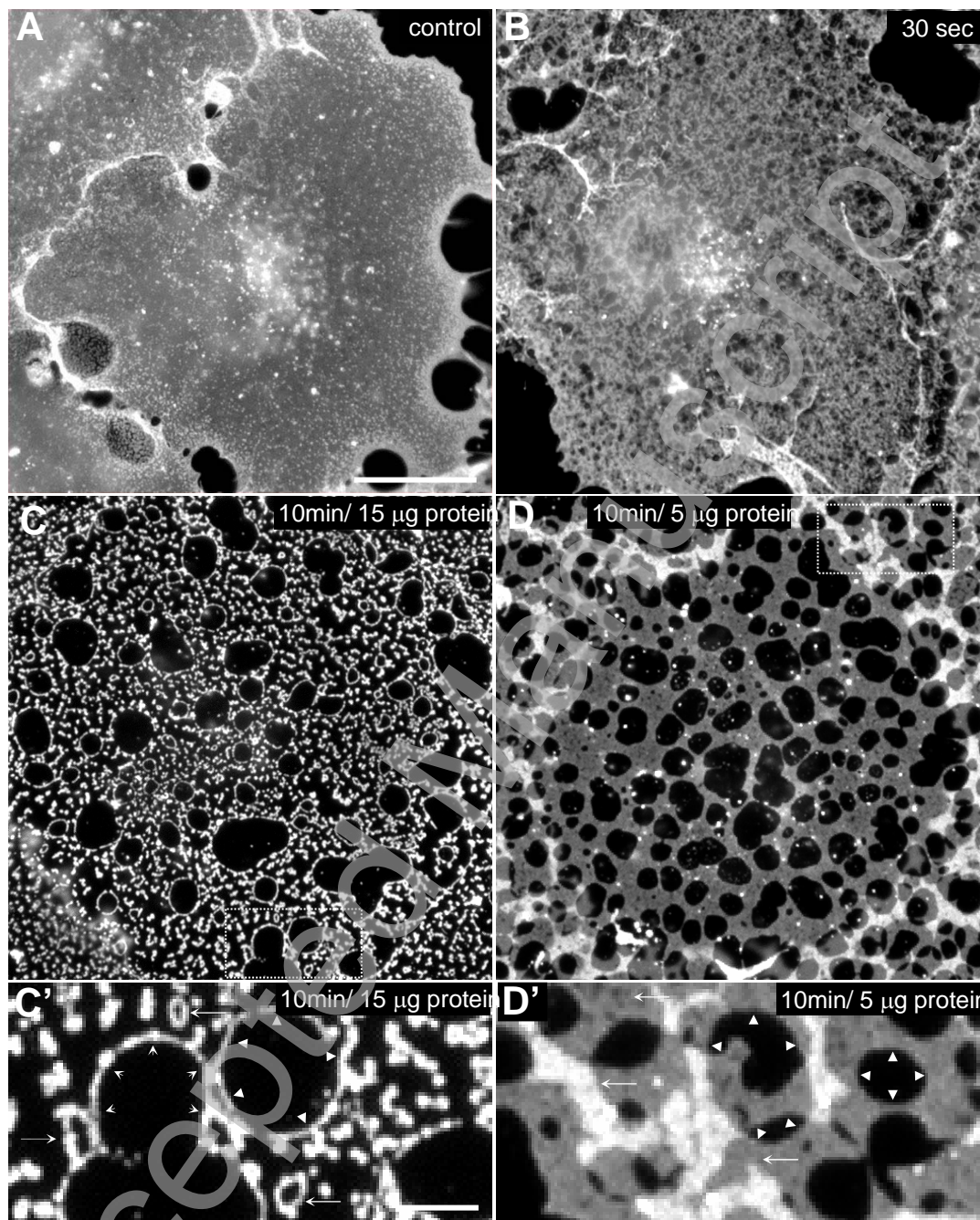
Ingelmo et al., figure 1

	-TX			
G	fluid population		condensed population	
	mean GP	coverage %	mean GP	coverage %
untreated cells	0.098	77.3	0.488	22.7
+10min (4ºC)	0.065	76.8	0.480	23.2

	+TX			
H	fluid population		condensed population	
	mean GP	coverage %	mean GP	coverage %
+20min (4ºC)	0.114	79.9	0.493	20.1
+10min 1%TX	0.079	48.6	0.639	51.4

Ingelmo et al., figure 2

Ingelmo et al., figure 3

Ingelmo et al., figure 4

Ingelmo et al., figure 5